Investigating the protective capacity of polymethylsiloxane polyhydrate against chromium (VI)-induced neurotoxicity of the rat optic nerve

O.V. Kuzenko [1], аспірантка; **Y.A. Dyomin** [1], д-р мед. наук, проф.; **E.V. Kuzenko** [2], д-р мед. наук, доцент

[1] Kharkiv Medical Academy of Postgraduate Education;
Kharkiv (Ukraine)

[2] Medical Institute of Sumy State Univercity;
Sumy (Ukraine)

E-mail: logvinenok26@gmail.com

Background: *Toxic optic neuropathy commonly develops in the presence of exogenous factors. With progression of the process, acute or chronic progressive death of retinal ganglion cells and their axons develops, leading to partial or total optic atrophy with visual function loss. Investigation of the effect of chromium (VI) on the optic nerve and evaluation of potential pathogenetic treatments of this effect are deemed relevant because of the global environmental crisis associated with pollution from chromium.*
Purpose: *To examine chromium (VI)-induced morphological changes in the rat optic nerve and to experimentally assess the efficacy of polymethylsiloxane polyhydrate (PMSPH) for correction of induced changes.*
Material and Methods: *Seventy two white outbred adult male rats were distributed in three groups (24 animals each) given water ad libitum. Animals in group 1 (a control group) were intact and given normal drinking water. Those in group 2 were given chromium (VI) (K2Cr2O7)-enriched (0.02 mol/L) drinking water but not Enterosgel. Animals in group 3 were given K2Cr2O7-enriched (0.02 mol/L) drinking water and treated with oral Enterosgel (0.8 mg/kg). Animals were decapitated under ether anesthesia and the intracranial optic nerve was harvested at three time points (20, 40 and 60 days after initiation of the experiment), and changes in the optic nerve were assessed by histomorphology and electron microscopy.*
Results: *Histomorphology found disrupted and fragmented nerve fibers, edematous connective tissue septa, and diffuse cellular gliosis in day-60 intracranial optic nerve specimens obtained from animals given chromium (VI)-enriched drinking water and not treated with Enterosgel. In addition, there was scanning electron microscopy evidence of electrolyte disbalance and accumulation of chromium (VI). Treatment with Enterosgel completely inhibited the effect of chromium (VI) on the rat optic nerve at days 20 and 40, and we observed only minimal consequences of discirculatory changes in day-60 specimens obtained from animals given chromium (VI)-enriched drinking water and treated with Enterosgel.*

Keywords:
chromium (VI), experiment, toxicity, optic nerve, Enterosgel, scanning electron microscope

Introduction

Heavy metal (HV) pollution is steadily increasing [1-4] and is a matter of serious concern because it can cause adverse effects on the environment and human health [5, 6]. Pollution accounts for 1 in every 7 deaths in low- and middle-income countries [7]. The top six pollutants (lead, radionuclides, mercury, chromium (VI), pesticides and cadmium) collectively affect the health of 95 million people in low and middle-income countries.

Vasyuta [8] reported that exposure to chromium (VI) is a major environmental factor for optic nerve atrophy (ONA), with at least twice maximum permissible concentration of chromium (VI) compounds found 1.79-times more frequently in water samples from the water basins in areas populated by patients with ONA than in water samples from the water basins in areas populated by controls.

The role of lead (Pb), mercury (Hg) and cadmium (Cd) in the development of glaucoma, cataract, age-related macular degeneration and dry eye disease has been stressed [9-12].

Interestingly, it has been reported that toxic optic neuropathy and retinopathy developed several years after implantation of the cobalt (II) and chromium (VI)-containing endoprosthesis [13-15]. The authors believe that the role of chromium (VI) is optic toxicity is not fully understood.

Advances in ophthalmology allow for developing animal models of ocular disorders (e.g. retinal and optic nerve disorders) induced by chronic exposure to various xenobiotics to elucidate the mechanisms of the onset and development of a particular pathology.

Investigating the substances that have the potential to reduce or prevent the toxic consequences of exposure of the body to heavy metals is believed to be promising. Studies on the effect of bee products, vitamins E, C, B1, probiotics, simvastatin and phyrochemicals on heavy metal toxicity are of particular scientific interest. Various remedies have been proposed for the treatment and prevention of heavy metal toxicity, but the issue is still controversial and further experimental evidence is needed.

Therefore, **the purpose** of this animal study was to examine chromium (VI)-induced morphological changes in the rat optic nerve and to experimentally assess the efficacy of polymethylsiloxane polyhydrate (PMSPH) for correction of induced changes.

Material and Methods

Seventy two white outbred adult male rats were distributed in three groups (24 animals each) given water ad libitum. Animals in group 1 (a control group) were intact and given normal drinking water. Those in group 2 were given chromium (VI) (K2Cr2O7)-enriched (0.02 mol/L) water which is characteristic for northern districts of Sumy region [16]. Animals in group 3 were given K2Cr2O7-enriched (0.02 mol/L) water ad libitum and treated with oral Enterosgel (0.8 mg/kg).

Particularly, the latter animals received orally, using a pipette, a single dose of 0.8 mg/kg/day of Enterosgel (PMSPH; manufacturer, KREOMA-FARM, Kyiv, Ukraine) at 9 AM, and were fasted for two hours thereafter, before being fed their diet. A recommended Enterosgel dose for humans is 46 mg/day. The Enterosgel dose for animals was calculated as per guidelines [17] and employing the formula proposed by Iu.R. Rybolovlev and R.S. Rybolovlev [18] in order to take into account the species of rats.

Animals were decapitated under ether anesthesia and the intracranial optic nerve was harvested. Changes in the optic nerve in the rats with induced toxic optic neuropathy, both treated and not treated with Enterosgel, were examined at three time points: 20, 40 and 60 days after initiation of the experiment.

The study was conducted in accordance with the principles stated in the Declaration of Helsinki and the European Convention for the Protection of Vertebrate Animals used for Experimental and other Scientific Purposes (Strasbourg, 1986).

Tissue samples were stained with hematoxylin and eosin (H&E) and examined under a Carl Zeiss Primo Star light microscope (Zeiss Primo Star™ Binocular 4X / 10X / 40X; Carl Zeiss Mycroscopy® GmbH, Gottingen, Germany) equipped with a Zeiss AxioCam ERc 5s digital camera.

As it is rather difficult to determine the type of optic nerve glial cells stained with H&E, we calculated the total number of glial cells on the slide, and converted this data into values expressed in mm2 in order to avoid a measurement error due to difference in the field of vision between different microscopes at the same magnification level. We used the following formula:

$$M=a/(10*n)$$

where *M* is the estimated number of cells per square millimeter;

a is a number of cells in the field of vision,

10 is the mean thickness of the slide cut assessed in millimeters,

n is ocular lens magnification.

Elelemental percent concentrations in the optic nerve were obtained using a CEM–102E scanning electron microscope (JCK Selmi, Sumy, Ukraine; accelerating voltage, 20-100 kV) equipped with an X-ray crystal diffraction spectrophotometer and energy dispersive X-ray spectrophotometer.

Magnified images (magnification, x2,700-x3,600) were processed by Kappa Image software (Kappa optoelectronics GmbH, Gleichen, Germany) and the digital camera Baumer/ Optronic Typ: CX 05c. Image mapping was performed and 'Quantmap' tool was used to improve further the quality of the elemental weight percent images produced

Variational statistics and Microsoft Excel 2007 software were used for analysis. Student's t-test was used to determine significance of differences. The level of significance $p \leq 0.05$ was assumed.

Results

Our histological studies revealed significant microstructural changes in the optic nerve in rats of experimental groups compared to controls (Fig. 1).

At day 20, initial degenerative changes were observed in glial cells of the optic nerve of animals given chromium (VI)-enriched water to drink: the nuclei appeared hyperchromic, chromatin aggregated into clumps, and nucleoli were mainly eccentrically arranged. Some cells occurred with individual light chromatin clumps scattered in the nucleus and at the peripheral nucleus (Fig. 1 B). Individual sites of poor circulation (dilated capillaries, red blood cell aggregates, sludge and white blood cell margination) were noted in the vessels of microcirculation bed in the optic nerve. Moderate perivascular edema surrounded the well-maintained vessel wall. The endothelial cells of the inner wall were irregularly shaped and had a basally located and indented nucleus.

At day 40, the changes became more apparent (Fig. 1 C). Histologically, the nerve fiber layer of the optic nerve was irregularly shaped and fragmented. Nerve fibers were separated from each other by edematous connective tissue septa and appeared wavy. Glial cells had indented outlines, their cellular and nuclear membranes were either not seen or poorly outlined, and nuclear chromatin was mildly stained.

At day 60, reactive neuroglial changes in the form of moderate glial cell proliferation were observed in rat optic nerve samples (Fig. 1 D). Some of these samples exhibited degenerative and necrotic changes which appeared similar

to melting sugar or as ghost cells. Apoptotic corpuscles observed in the field of vision of the light microscope were corresponded to the final stage of glial cell apoptosis. There was disruption of the intracranial optic nerve with numerous but not large-scale deformations and loss of parallel arrangement of optic nerve filaments.

Specimens of group 2 showed changes in the estimated number of optic nerve glial cells per mm2 at all the three time points (Table 1). The most apparent changes (with the estimated number of optic nerve glial cells per mm2 as large as 3,060 ± 180; a 1.7-fold increase compared to controls, $p = 0.02$) were observed at day 60.

Enterosgel-treated (i.e., group 3) animals showed reduced morphological changes in the optic nerve neuroglia and ganglion axons compared to group 2 rats that were watered with chromium (VI) water and not treated with Enterosgel (Figs 2A, B).

Microscopic study of histological optic nerve specimens obtained from group 3 rats at days 20 and 40 revealed reactive transformations in the nerve fibers and neuroglial cells (Figs 2A, B). Visualization of the clear parallel arrangement of optic nerve filaments was somewhat hampered by mild edema of connective tissue septa which included collagen, elastic and reticular fibers, fibroblasts numerous blood vessels. Individual degenerated glial cells with pericellular edema were occasionally seen (Figs 2B, 3).

Optic nerve specimens obtained from group 3 rats at day 60 exhibited more apparent morphological changes (Figs 2C). By optic microscopy, the nerve layer appeared as a meshwork of tortuous and disarranged nerve filaments due to increased edematous changes in the connective tissue covering the bundles of optic nerve filaments.

At day 60, the estimated number of optic nerve glial cells per mm2 in the optic nerve specimens of Enterosgel-treated animals given chromium (VI)-enriched water to drink was 1890 ± 90 ($p \geq 0.05$), i.e., almost the same as in controls (1800 ± 60, $p \geq 0.05$; Table 1), but the glial cells from group 3 specimens had mild degenerative changes. Individual glial cells in the process of phagocytosis by macrophages were occasionally seen.

Table 2 presents the results of quantitative microelement analysis for the intracranial optic nerve of experimental groups of rats by scanning electron microscopy with an X-ray crystal diffraction spectrometer and energy dispersive X-ray spectrometer.

There was no accumulation of chromium (VI) in the group 2 specimens obtained at day 20. However, the percentage of chromium (VI) in the group 2 specimens substantially increased with time, to 0.13 ± 0.01 ($p \geq 0.05$) by day 40, and 9.46-fold to 1.23 ± 0.1% ($p \leq 0.02$) by day 60 (Table 2).

Quantitative X-ray microanalysis optic nerve specimens (particularly, group 2 specimens obtained at 60 days) was performed using an electron microscope equipped with an energy dispersive X-ray spectrometer. Fig. 3 presents relevant EDS spectra.

Elemental mapping of group 2 specimens obtained at day 60 was performed to verify accumulation of chromium (VI) at this time point (Fig. 4). The map of the distribution of elements (Fig. 4B) was overlapped with the optic nerve microstructure image (Fig. 4A) to obtain green grains corresponding to chromium (VI), red grains corresponding to carbon (C), violet grains corresponding to phosphorus (P), and turquoise blue grains corresponding to oxygen (O) (Fig. 4C). Fig. 4B shows that the site of accumulation of chromium (VI) is in the perineural space of the optic nerve, and there is chromium diffusion to neural filaments.

In addition to chromium (VI), there was a substantial difference in Ca2+, Mg2+, and Na2+, but not in other microelements found by X-ray microanalysis of group 2 specimens, between the latter specimens and group 1 (i.e., control) specimens (Table 2). There was a stable tendency to decrease in the percentage of Ca2+ in group 2 specimens with time, with 4.43 ± 0.73% ($p \geq 0.05$) at day 20, and 3.75 ± 0.91% ($p \leq 0.05$) at day 60, compared to 4.56 ± 0.79% ($p \geq 0.05$) for control specimens. The tendency to increase in the percentage of Mg2+ in group 2 specimens with time was unstable, with 0.12 ± 0.01% ($p \geq 0.05$) at day 20, 0.13 ± 0.04% ($p \geq 0.05$) at day 40, and 0.06 ± 0.009% ($p \geq 0.05$) at day 60, compared to 0.10 ± 0.03% ($p \geq 0.05$) for control specimens. The pattern of changes in Na2+ in group 2 specimens with time was quite opposite to the pattern of changes in Ca2+. The percentage of Nag2+ in group 2 specimens steadily increased with time, and was 0.25 ± 0.06% ($p \leq 0.05$) at day 60, compared to 0.12 ± 0.02% ($p \geq 0.05$) for control specimens.

X-ray microanalysis of group 3 (chromium plus Enterosgel) specimens of the optic nerve showed that hexavalent Cr was present only at the final time point, day 60 (at a percentage of 0.26 ± 0.05%, $p \geq 0.05$), but not at the previous time points, day 20 and day 40 (Table 2). In addition, we failed to identify hexavalent Cr at the element distribution map for group 3 specimens obtained at day 40 (Fig. 5), which confirmed the above finding.

Percentages of Ca2+, Mg2+ and Nag2+ in group 3 optic nerve specimens obtained at days 40 and 60 but not day 20 were different from percentages of Ca2+, Mg2+ and Nag2+ for the control group specimens. The percentage of Fe2+ in group 3 optic nerve specimens obtained at day 20 was 0.17 ± 0.08%, which was 30.76% ($p \geq 0.05$) higher than the percentage in the control group specimens (Table 2).

Discussion

Here, we for the first time conduct a study that examines the protective effect of Enterosgel on hexavalent Cr-induced optic nerve neurotoxicity in rats. The nerve fibers exhibited deformation and fragmentation, were separated from each other by edematous connective tissue septa, and there was diffuse cellular gliosis and scanning electron microscopy evidence of electrolyte disbalance and accumulation of hexavalent Cr in day-60 intracranial optic nerve specimens obtained from animals given

chromium (VI)-enriched drinking water and not treated with Enterosgel. Enterosgel treatment for chromium (VI)-induced optic nerve neurotoxicity resulted in a decrease in toxic effect of chromium (VI) on the optic nerve at days 20 and 40, with only consequences of discirculatory changes in the form of mild edema of collagen fibers in between the deformed filaments of the optic nerve at day 60.

Our histopathological findings are in partial agreement with findings of a study by Salama and colleagues [19] who investigated the distribution and the effects of Cr in both brain and lung following the intranasal instillation of potassium dichromate (inPDC) in rats. The findings revealed that the toxic manifestations were directly proportional to the delivered concentration of Cr to the tissue. Brain of inPDC (0.5 mg/kg)-treated rats showed signs of focal gliosis and degeneration of individual neuronal cells associated with neuronophagia. Brain of inPDC (2 mg/kg)-treated rats revealed the most severe histopathological lesions, compared to other treated groups. These lesions were manifested by neuronal cell necrosis, proliferation of glia cells, satellatosis and extensive hemorrhage.

In the current study, morphological changes were confirmed by scanning electron microscopy evidence of the presence of chromium in the optic nerve of rats exposed to drinking water supplemented with K2Cr2O7 at all time points of the experiment. This may be explained by the capacity of hexavalent Cr to pass the brain-blood barrier [20].

Metabolic pathways and toxicity of chromium depend on whether it is hexavalent or trivalent chromium. Chromium (VI) compounds have been reported to be more toxic than chromium (III) compounds [21]. Once inside the cells, chromium (VI) can be reduced to its lower oxidation states, chromium (V), chromium (IV), and chromium (III), with formation of numerous reactive oxygen species (ROS) due to block of the mitochondrial respiratory chain complex I [22], and ROS can cause damage to cellular proteins, lipids and DNA [23]. However, under physiological conditions, ROS are inactivated by the atioxidative system [24]. A chromium (VI)-induced decrease in the activity of the atioxidative system leads to a condition known as oxidative stress (OS) [25-27]. Oral administration of potassium dichromate resulted in oxidative stress in rabbits, with significant decreases in the levels of glutathione peroxidase and superoxide dismutase, and catalase activity, and an increase in the level of malondialdehyde, a final product of lipid peroxidation [28].

Our findings of apoptotic changes in glial cells of the optic nerve in rats exposed to drinking water supplemented with chromium (VI) can be explained by previous studies. Xiao and colleagues [22] demonstrated that chromium (VI) induced the activation of caspase-3, an irreversible stage in the internal (mitochondrial) pathway of apoptosis. Similar to other cationic metals, chromium (VI) crosses the external mitochondrial membrane through molecular mimicry [29, 30]. Because many astrocyte functions, such as ion and neurotransmitter transport, are energy demanding [31], mitochondrial dysfunction can impair the ability of astrocytes to carry out neuroprotective functions. Oligodendrocyte dysfunction or apoptosis results in demyelination, leading to the impaired conduction of nerve impulses. Low subtoxic doses of Cu2+, Cr3+, Ni2+, Co2+, Pb2+, Cd2+, and Al3+, incubated with oligodendrocytes for 24 h, produced reduced cell viability levels and reduced levels of lipids in oligodendrocytes [32]. Long-term exposure to high concentrations of heavy metals have been for long associated with several neurological disorders such as multiple sclerosis, Parkinson's disease, Alzheimer's disease and muscular dystrophy [33].

In the current study, the enterosorbent Enterosgel was selected as a potential treatment to improve neurotoxicity associated with exposure to chromium in drinking water. Enterosgel has been reported to prevent the development of oxidative stress in mitochondria [34] and to adsorb toxic substances from the gastrointestinal lumen, thus blocking their passage from the lumen to the systemic circulation [35].

The current study for the first time demonstrated that treatment with Enterosgel resulted in an improvement in chromium (VI)-induced pathomorphological changes in the rat optic nerve. This was evidenced by longitudinal morphological changes and X-ray spectral analysis. Particularly, treatment with Enterosgel completely inhibited the effect of chromium (VI) at days 20 and 40. Qualitative and quantitative changes in the toxic effect of chromium on the optic nerve were found at day 60, which may indicate the disruption of the body's compensatory capacity.

Based on the results of morphological and electron microscopy studies, we conclude that treatment with Enterosgel at a dose of 45 mg/kg resulted in complete prevention of chromium (VI)-induced alteration processes in the rat optic nerve for the first 40 days of the experiment.

Recommendation for practitioners: Treatment with Enterosgel can be used as part of the multicomponent treatment of optic nerve toxicity.

References

1. Tong S, Li H, Wang L, Tudi, M. Concentration, Spatial Distribution, Contamination Degree and Human Health Risk Assessment of Heavy Metals in Urban Soils across China between 2003 and 2019 - A Systematic Review. Int J Environ Res Public Health. 2020 Apr 29;17(9):3099. doi: 10.3390/ijerph17093099.
2. Tytła M. Assessment of Heavy Metal Pollution and Potential Ecological Risk in Sewage Sludge from Municipal Wastewater Treatment Plant Located in the Most Industrialized Region in Poland-Case Study. Int J Environ Res Public Health. 2019 Jul 9;16(13):2430. doi: 10.3390/ijerph1613243.
3. Stetsenko DO, Dolin VV. [Heavy metals in soils of radiocontaminated forest environmental systems]. Poshukova ta ekologichna geokhimiia. 2009;9:42-7. Ukrainian.
4. Biletska EM, Onul NM, Golovkova TA, et al. [Environment- and hygiene-based determinacy of deterioration of health for population of industrial region]. 2016;4:14-8. Ukrainian.

5. Rahman Z, Singh VP. The relative impact of toxic heavy metals (THMs) (arsenic (As), cadmium (Cd), chromium (Cr(VI)), mercury (Hg), and lead (Pb)) on the total environment: an overview. Environ Monit Assess. 2019 Jun 8;191(7):419. doi: 10.1007/s10661-019-7528-7.
6. Junaid M, Hashmi MZ, Malik RN, et al. Toxicity and oxidative stress induced by chromium in workers exposed from different occupational settings around the globe: A review. Environ Sci Pollut Res Int. 2016 Oct;23(20):20151-20167. doi: 10.1007/s11356-016-7463-x.
7. World's Worst Pollution Problems 2015. Available at:https://www.greencross.ch/wp-content/uploads/uploads/media/pollution_report_2015_top_six_wwpp.pdf
8. Vasyuta VA. [Medical and social substantiation of the system of medical care for patients with optic nerve atrophy]. [Extended Abstract of Dissertation for the Degree of Dr Sc (Med)]. Kyiv, 2015. Ukrainian.
9. Vennam S, Georgoulas S, Khawaja A, et al. Heavy metal toxicity and the aetiology of glaucoma. Eye (Lond). 2020 Jan; 34(1):129-37. doi: 10.1038/s41433-019-0672-z.
10. Lin S-C, Singh K, Lin SC. Association Between Body Levels of Trace Metals and Glaucoma Prevalence. JAMA Ophthalmol. 2015 Oct;133(10):1144-50. doi: 10.1001/jamaophthalmol.2015.2438.
11. Jung SJ, Lee SH. Association between Three Heavy Metals and Dry Eye Disease in Korean Adults: Results of the Korean National Health and Nutrition Examination Survey. Korean J Ophthalmol. 2019 Feb;33(1):26-35. doi: 10.3341/kjo.2018.0065.
12. Wills NK, Kalariya N, Sadagopa Ramanujam VM, et al.. Human retinal cadmium accumulation as a factor in the etiology of age-related macular degeneration. Exp Eye Res. 2009; 89: 79-87. doi: 10.1016/j.exer.2009.02.014.
13. Apel W, Stark D, Stark A, et al. Cobalt-chromium toxic retinopathy case study. J Doc Ophthalmol. 2013 Feb;126(1):69–78. doi: 10.1007/s10633-012-9356-8.
14. Ng SK, Ebneter A, Gilhotra JS. Hip-implant related chorio-retinal cobalt toxicity. Indian J Ophthalmol. Jan-Feb 2013;61(1):35-7. doi: 10.4103/0301-4738.105053.
15. Garcia MD, Hur M, Chen JJ, et al. Cobalt toxic optic neuropathy and retinopathy: Case report and review of the literature. Am J Ophthalmol Case Rep. 2020 Jan 25;17:100606. doi: 10.1016/j.ajoc.2020.100606.
16. Vashkulat NP. Establish levels of heavy metals in soils in Ukraine. Environ Health. 2002;2:44–6.
17. Enterosgel reference data: https://compendium.com.ua/info/45247/enterosgel_/?gclid=Cj0KCQiAhs79BRD0ARIsAC6XpaWNtWnGca92BMToa94LSBYTztnf8rHzcqgqIYuDB5J18_1AkqghI7gaAvxTEALw_wcB
18. Rybolovlev IuR, Rybolovlev RS. [Dosing substances for mammals based on biological activity constants]. Doklady Akademii Nauk SSSR. 1979;247(6):1513-6. Russian.
19. Salama A, Hegazy R, Hassan A. Intranasal Chromium Induces Acute Brain and Lung Injuries in Rats: Assessment of Different Potential Hazardous Effects of Environmental and Occupational Exposure to Chromium and Introduction of a Novel Pharmacological and Toxicological Animal Model. PLoS One. 2016; 11(12): e0168688. doi: 10.1371/journal.pone.0168688.
20. Duckett S. Abnormal deposits of chromium in the pathological human brain. J Neurol Neurosurg Psychiatry. 1986 Mar; 49(3): 296–301. doi: 10.1136/jnnp.49.3.296.
21. Fang Z, Zhao M, Zhen H, et al. Genotoxicity of tri- and hexavalent chromium compounds in vivo and their modes of action on DNA damage in vitro. PLoS One. 2014 Aug 11;9(8):e103194. doi:10.1371/journal.pone.0103194.
22. Xiao F, Li Y, Dai L, et al. Hexavalent chromium targets mitochondrial respiratory chain complex I to induce reactive oxygen species-dependent caspase-3 activation in L-02 hepatocytes. Int J Mol Med. 2012 Sep;30(3):629-35. doi: 10.3892/ijmm.
23. Sun H, Brocato J, Costa M. Oral Chromium Exposure and Toxicity. Curr Environ Health Rep. 2015 Sep;2(3):295-303. doi: 10.1007/s40572-015-0054-z.
24. Velichkovskiĭ BT. Vestn Ross Akad Med Nauk. 2001;(6):45-52. [Free radical oxidation as a link of early and prolonged adaptation to environmental factors]. Russian.
25. Kurutas EB. The importance of antioxidants which play the role in cellular response against oxidative/nitrosative stress: current state. Nutr J. 2016 Jul 25;15(1):71. doi: 10.1186/s12937-016-0186-5.
26. Kotyzová D, Hodková A, Bludovská M, et al. Effect of chromium (VI) exposure on antioxidant defense status and trace element homeostasis in acute experiment in rat. Toxicol Ind Health. 2015 Nov;31(11):1044-50. doi: 10.1177/0748233713487244.
27. Patlolla AK, Barnes C, Yedjou C, et al. Oxidative stress, DNA damage, and antioxidant enzyme activity induced by hexavalent chromium in Sprague-Dawley rats. Environ Toxicol. 2009;24(1):66-73. doi: 10.1002/tox.20395.
28. Mary Momo CM, Ferdinand N, Omer Bebe NK, et al. Oxidative Effects of Potassium Dichromate on Biochemical, Hematological Characteristics, and Hormonal Levels in Rabbit Doe (Oryctolagus cuniculus). Vet Sci. 2019 Mar;6(1):30. doi: 10.3390/vetsci6010030.
29. Bucio L, García C, Souza V. Uptake, cellular distribution and DNA damage produced by mercuric chloride in a human fetal hepatic cell line. Mutat Res. 1999 Jan 25;423(1-2):65-72. doi: 10.1016/s0027-5107(98)00226-7.
30. Castellino N, Aloj S. Intracellular distribution of lead in the liver and kidney of the rat. Br J Ind Med. 1969 Apr;26(2):139-43. doi: 10.1136/oem.26.2.139.
31. Hertz L, Dienel GA. Lactate transport and transporters: general principles and functional roles in brain cells. J Neurosci Res. 2005 Jan 1-15;79(1-2):11-8. doi: 10.1002/jnr.20294.
32. Maiuolo J, Macrì R, Bava I, et al. Myelin Disturbances Produced by Sub-Toxic Concentration of Heavy Metals: The Role of Oligodendrocyte Dysfunction. Int J Mol Sci. 2019 Sep 14;20(18):4554. doi: 10.3390/ijms20184554.
33. Chin-Chan M, Navarro-Yepes J, Quintanilla-Vega B. Environmental pollutants as risk factors for neurodegenerative disorders: Alzheimer and Parkinson diseases. Front Cell Neurosci. 2015 Apr 10;9:124. doi: 10.3389/fncel.2015.00124.
34. Nikolaiev VG, Klishch IM, Zhulkevich IV. [Using Enterosgel for prevention of oxidative stress in acute blood loss]. Visnyk naukovykh doslidzhen. 2009;8:72-4. Ukrainian.
35. Howell CA, Mikhalovsky SV, Markaryan EN, et al. Investigation of the adsorption capacity of the enterosorbent Enterosgel for a range of bacterial toxins, bile acids and pharmaceutical drugs. Sci Rep. 2019;9:5629.

The authors declare no conflict of interest which could influence their opinions on the subject or the materials presented in the manuscript.

Table 1. Mean values for neuroglial cell numbers in the intracranial optic nerve for the three study groups of rats

Group	Time point after initiation of the experiment	Neuroglial cell number in 1 mm²
Group I (K) (n =24)	controls	1800±60
Group II (Cr) (n =24)	Day 20	2010±210
	Day 40	2310±270*
	Day 60	3060±180**
Group III (Cr +E) (n =24)	Day 20	1680±90
	Day 40	1710±60
	Day 60	1890±90

Note: *p ≤ 0.05 (t-test) and **p ≤ 0.02 (t-test), statistically significant differences with controls; (Cr), a group of rats given chromium (VI)-enriched drinking water but not Enterosgel; (Cr +E), a group of rats given both chromium (VI)-enriched drinking water and Enterosgel

Table 2. Changes in percentages of chemical elements in the intracranial optic nerve for groups of study rats based on the results of micro x-ray spectrum analysis

Group	Time point	Elements under study,%				
			O	P	Ca	S
Group 1 (control group) (n =24)	baseline	50.47±2.76	32.72±1.24	14.85±1.34	4.56±0.79	2.3±0.09
Group 2(Cr) (n =24)	Day 20	50.43±3.31	32.62±1.35	14.7±1.98	4.43±0.73	2.7±0.1
	Day 40	50.36±2.24	32.56±1.38	14.91±1.48	4.23±0.86	2.5±0.15
	Day 60	49.23±3.47	32.65±2.12	14.4±1.56	3.75±0.91*	2.4±0.87
Group 3 (Cr +E) (n =24)	Day 20	51.34±2.49	32.71±1.98	14.57±1.23	4.75±0.47	2.4±0.13
	Day 40	50.56±3.21	33.57±1.56	13.47±0.97	3.23±1.15*	2.7±.0.79
	Day 60	50.35±2.48	32.44±2.23	14.91±0.94	3.97±1.27*	2.2±0.93

Group	Time point	Elements under study,%					
			Mg	K	Cl	Na	Cr
Group 1 (control group) (n =24)	baseline	0.13±0.03	0.10±0.03	0.08±0.01	0.15±0.03	0.12±0.02	-
Group 2(Cr) (n =24)	Day 20	0.14±0.04	0.12±0.01	0.1±0.03	0.17±0.06	0.13±0.05	-
	Day 40	0.15±0.03	0.13±0.04	0.1±0.02	0.2±0.09	0.23±0.09*	0.13±0.01
	Day 60	0.13±0.06	0.06±0.009	0.07±0.01	0.16±0.01	0.25±0.06*	1.23±0.1**
Group 3 (Cr +E) (n =24)	Day 20	0.17±0.08	0.12±0.04	0.1±0.009	0.2±0.04	0.12±0.07	-
	Day 40	0.14±0.05	0.12±0.04	0.1±0.009	0.18±0.08	0.12±0.04	-
	Day 60	0.12±0.09	0.10±0.06	0.09±0.01	0.15±0.09	0.15±0.06	0.26±0.05

Note: *p≤0.05; **p≤0.02, significant difference compared to controls; (Cr), a group of rats given chromium (VI)-enriched drinking water but not Enterosgel; (Cr +E), a group of rats given both chromium (VI)-enriched drinking water and Enterosgel

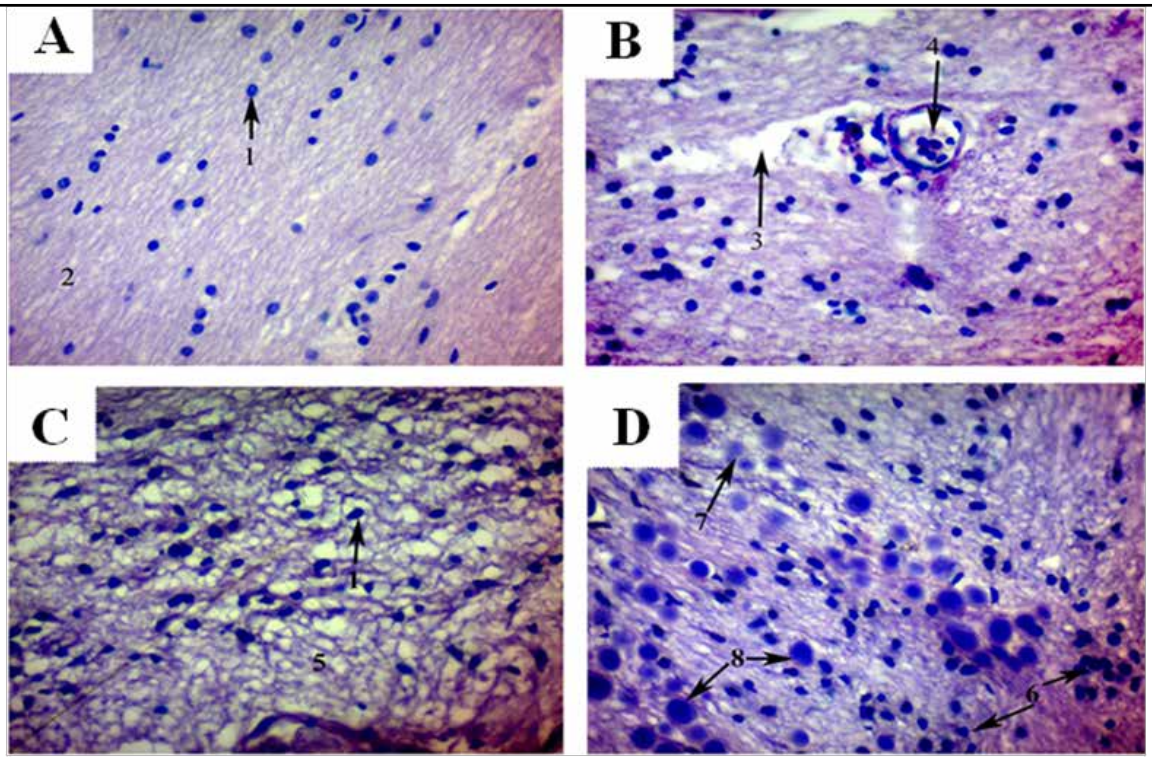

Fig. 1. Longitudinal sections of rat optic nerve specimens obtained from controls (A) and group 2 rats (given chromium (VI)-enriched drinking water but not treated with Enterosgel) at days 20 (B), 40 (C) and 60 (D). Hematoxylin and eosin staining, original magnification, x400. Notes: 1, glial cell; 2, nerve filaments; 3, perivascular edema; 4, dilated and obstructed vessels; 5, edema in between disorganized nerve filaments; 6, gliotic phenomena; 7, apoptotic and degenerative changes in glial cells; 8, necrotic and degenerative changes in glial cells.

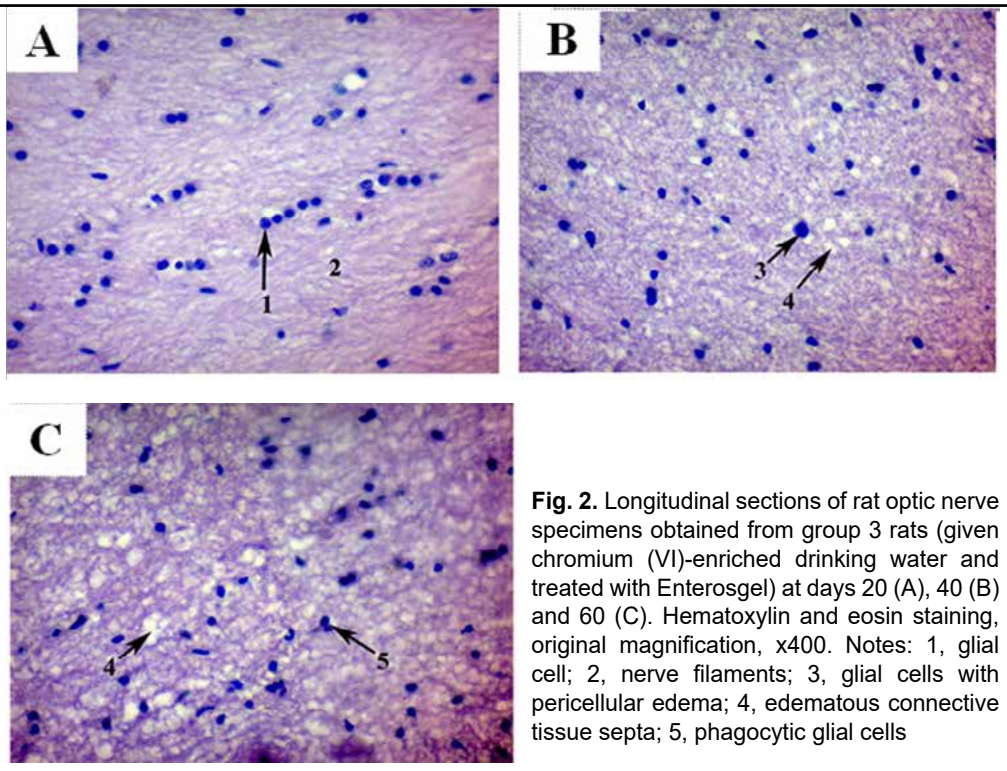

Fig. 2. Longitudinal sections of rat optic nerve specimens obtained from group 3 rats (given chromium (VI)-enriched drinking water and treated with Enterosgel) at days 20 (A), 40 (B) and 60 (C). Hematoxylin and eosin staining, original magnification, x400. Notes: 1, glial cell; 2, nerve filaments; 3, glial cells with pericellular edema; 4, edematous connective tissue septa; 5, phagocytic glial cells

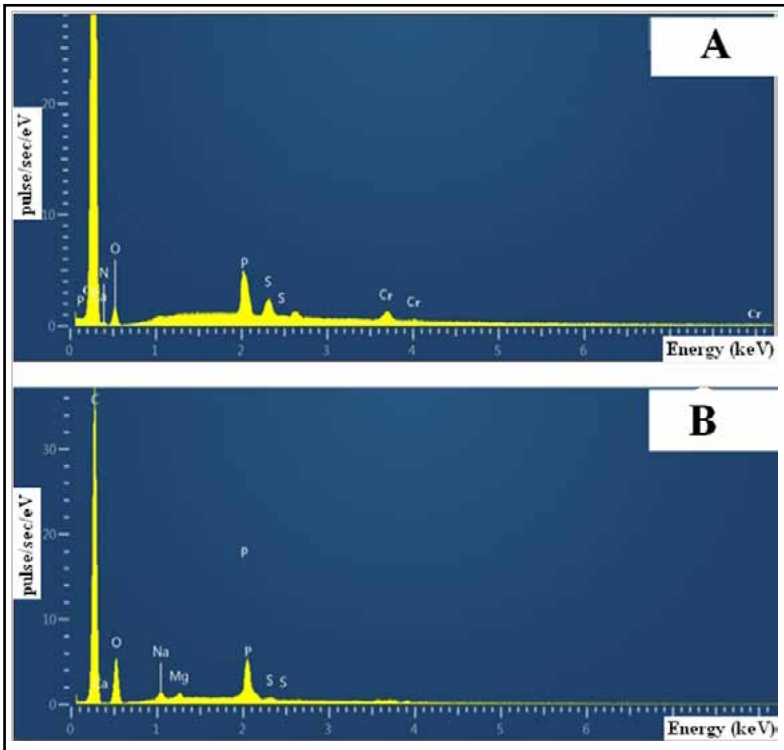

Fig. 3. Energy-dispersive x-ray spectra of rat optic nerve specimens obtained from group 2 rats at day 60 (A) and group 3 rats at day 40 (B)

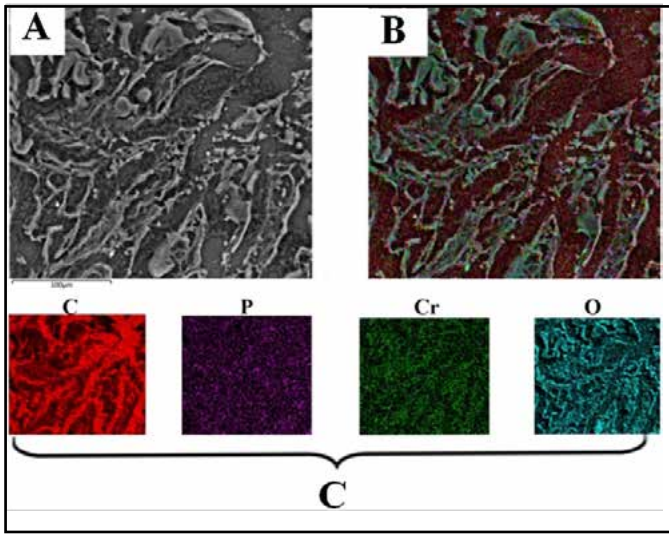

Fig. 4. Energy-dispersive micro x-ray analysis (accelerating voltage, 20 kV) of rat optic nerve specimens obtained from group 2 rats at day 60. Original magnification, x200. (A) Microstructure of the optic nerve. (B) Profile of element distribution on the surface. (C) EDX elemental mapping for carbon (C), phosphorus (P), chromium (Cr), and oxygen (O)

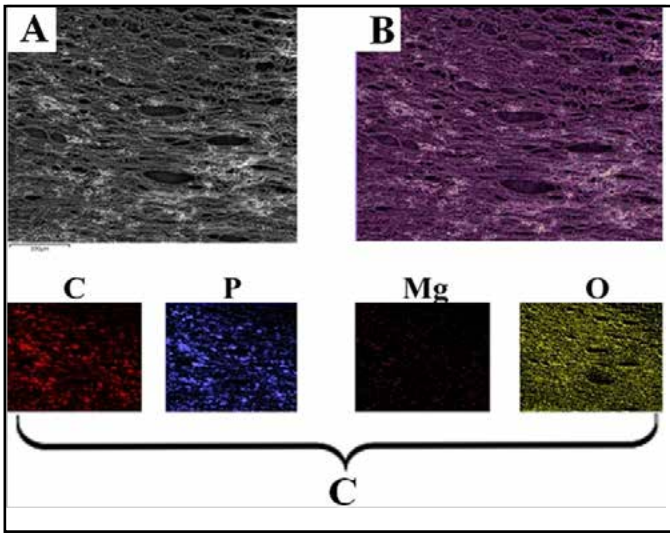

Fig. 5. Energy-dispersive micro x-ray analysis (accelerating voltage, 20 kV) of rat optic nerve specimens obtained from group 3 rats at day 40. Original magnification, x200. (A) Microstructure of the optic nerve. (B) Profile of element distribution on the surface. (C) EDX elemental mapping for carbon (C), phosphorus (P), magnesium (Mg), and oxygen (O)